LUNAR THERMAL NEUTRON EMISSION MAPPED BY THE LRO/LEND DOPPLER DETECTORS.

T. A. Livengood[1], G. Chin[2], I. G. Mitrofanov[3], W. V. Boynton[4], D. Hamara[4], K. P. Harshman[4], M. L. Litvak[3], T. P. McClanahan[2], R. Z. Sagdeev[6], A. B. Sanin[3], R. D. Starr[7], J. J. Su[6] [1]CRESST/U. of MD, Code 693, NASA/GSFC, Greenbelt, MD 20771, timothy.a.livengood@nasa.gov, [2]NASA/GSFC, [3]Institute for Space Research, Moscow, Russia, [4]Lunar and Planetary Lab, U of AZ, [5]Computer Sciences Corp., [6]Dept. of Physics, U. of MD, [7]Dept. of Physics, Catholic U. of America.

Introduction: The Lunar Reconnaissance Orbiter (LRO) Lunar Exploration Neutron Detector (LEND) comprises multiple detector systems, including the sensor for epithermal neutrons (SETN), the collimated sensors for epithermal neutrons (CSETN), the sensor for high-energy neutrons (SHEN), and three sensors for thermal neutrons (STN1, STN2, and STN3) [1]. Thermal neutron emission fluxes respond strongly to the presence of high atomic number species (e.g., iron), which deplete the emission of low-energy neutrons. The lunar maria and South Pole Aitken Basin regions, which are known to be iron-rich, thus feature the least thermal neutron fluxes on the Moon [2-4].

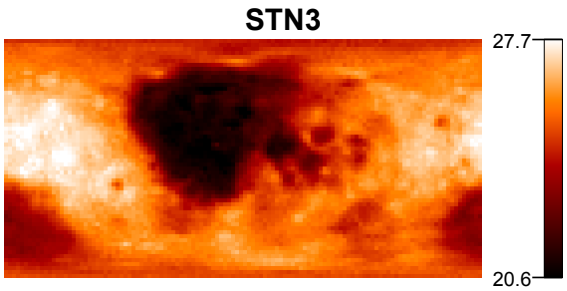

Fig. 1: Cylindrical-projection map of lunar thermal neutron emission measured by LEND STN3 sensor, calibrated in neutron detection rate per second. Maria form the darkest region on the Moon, with a dark region over South Pole Aitken Basin as well, both due to high iron content [3]

Two of the thermal neutron detectors, STN1 and STN2, form a paired set of Doppler detectors, while the STN3 sensor operates as a standalone detector, where the sensor roles and the identity of the detected neutron flux are distinguished by location of the sensor on the nadir-pointed LEND housing [1]. STN3 is at the apex of the collimator structure with a mostly unobstructed field of view that is filled by the Moon. Sensitivity nominally extends to the lunar horizon but is limited by anisotropic emission of neutron flux, which falls off as roughly a cosine dependence from the local surface normal. STN3 includes a relatively small but significant background detection rate due to neutrons generated within neighboring metal parts by galactic cosmic ray (GCR) impacts on the instrument and spacecraft structure. STN3 includes a large contribution of epithermal neutron detections in addition to the thermal neutron flux that is the purpose for the detector. This unwanted contribution can be subtracted by appropriately scaling and subtracting the epithermal neutron flux measured by the SETN detector [4].

The Doppler detectors, STN1 and STN2, are designed to provide an alternative technique to remove spacecraft background and unwanted epithermal neutron flux. The detectors are mounted on the exterior base of the collimator housing, which is highly opaque to thermal-energy neutrons, with one detector mounted in the direction of spacecraft motion and one following [1, 4]. Low energy neutrons move sufficiently slowly that they are unable to catch up to the following detector, but can be detected by the forward-mounted detector plowing into them. Higher-energy neutrons reach both detectors, and background fluence generated within the instrument and spacecraft structures is in the rest frame of the sensors and thus reaches them with uniform sensitivity. In principle, subtracting the following detector's measured flux from the forward detector's measured flux should eliminate background and epithermal neutron flux, resulting in a measurement of only the low-energy thermal neutron population without background signal. Empirically, there is evidence for an additional background that must be subtracted, which is the purpose of the present work.

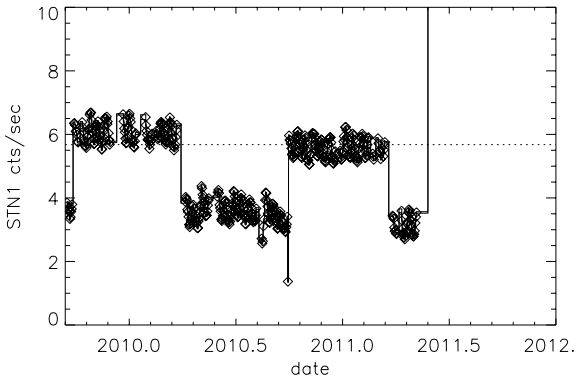

Fig. 2: Absolute value of STN1 minus STN2, averaged over daily LEND data sets until an instrument event resulted in deactivating the sensors around mid-2011. The discontinuities result from switching the spacecraft orientation.

Every few months, the spacecraft switches its orientation relative to the direction of motion, swapping which detector is forward and which is reverse. The difference STN1–STN2 thus switches its sign, as the forward detector always experiences a significantly greater neutron detector rate. As seen in Fig. 2, the diurnal average of the difference in detector counts per second exhibits a square wave as well as a slight decline in absolute signal level and in the square wave amplitude. All neutron flux sources that contribute to measured flux are due to GCR impact on lunar or spacecraft materials, accounting for the declining signal during changing solar activity, shielding out GCR flux during the approach to solar maximum. The square wave amplitude is of order 10% of the count rate in the individual detectors, which is too great to be accounted for by differences in sensitivity – sensor sensitivity is primarily controlled by ^{3}He gas pressure within the proportional counter chamber, which can be determined to significantly greater precision than 10%. The difference between the detectors appears to be due to the fact that STN1 is exposed to neutron flux generated in the body of the spacecraft itself, while STN2 is shielded from the spacecraft by the collimator, resulting in a different background fluence available to each detector.

This work will estimate the additional background fluence in the STN1 detector to enable creating a high-quality map of thermal neutron flux on the Moon from the differential Doppler measurement. This map will be compared with mapped thermal neutron flux from the omnidirectional detector data sets from the Lunar Prospector (LP) thermal neutron detector [3], and the LEND STN3 omnidirectional detector [4] to investigate background and to search for other systematic effects in the sensor systems.

References: [1] Mitrofanov *et al.* (2010) *Science* **330**, 483–486. [2] Litvak et al. (2012) *JGR-Planets* **117**, E00H22, doi: 10.1029/2011JE003949. [3] Feldman et al. (1998) *Science* **281**, 1489–1493, doi: 10.1126/science.281.5382.1489. [4] Livengood *et al.* (2018) *P&SS* in press, doi: 10.1016/j.pss.2017.12.004.